

Cascaded Filter for the LWA Antenna

Whitham D. Reeve

1. Introduction

The Long Wavelength Array antenna [{ReeveLWA}](#) has a design frequency range from about 5 to 90 MHz. The FM broadcast band from 88 to 108 MHz can cause interference at all but the most remote locations, so the usable upper frequency is somewhat below 88 MHz. At the other end of the antenna's frequency range, but below it, is the AM broadcast band from 535 to 1705 kHz. Although not in the LWA frequency range, AM broadcast stations generally use high-power transmitters and could cause receiver overload even if located far from the antenna.

To limit interference from these broadcast bands to the receivers connected to the LWA antenna, a filter has been designed with a passband from 5 to 80 MHz (figure 1). The filter is a composite made from a cascade of three separate commercial filter modules (figure 2). The filter is designated model FL590, which indicates the filter modules used for the band edges. I previously produced articles on basic filters and filter measurements at [{ReeveBasFilt}](#) and [{ReeveFilt}](#), respectively, and these should be referenced for background information. It should be noted that this filter reduces interference to a receiver but not to the active components in the LWA antenna itself.



Figure 1 ~ FL590 filter ready for use. The filter components are housed in a milled aluminum enclosure with an SMA-female connector on each end. The enclosure is repurposed from an AEL bandpass filter. Dimensions are 120 L x 35 W x 27 H mm. Image © 2020 W. Reeve



Figure 2 ~ Three shielded, surface mounted, lumped element filters installed on an in-house designed printed circuit board. From left-to-right, Mini-Circuits SXHP-5+ highpass filter, BSF-C100+ bandstop filter and SXLP-90+ lowpass filter. Tinned copper pigtail terminals can be seen at each end for soldering to the SMA connectors mounted on the enclosure. The PCB dimensions are 115 L x 30 W x 8 H mm, including the filter modules. Image © 2020 W. Reeve

The remainder of this article describes the filter design (section 2), the printed circuit board used in the filter (section 3), filter simulation using free software and measurements with a professional vector network analyzer (section 4), comparative measurements with an amateur vector network analyzer (section 5), filter performance

when connected to an outdoor test antenna (section 6) and applications of the filter in up-converters to be used with the LWA antenna and the e-Callisto solar radio spectrometer project (section 7). Conclusions (section 8) and weblinks and references (section 9) also are provided.

2. Filter Design

My goals were to design a filter having a passband of 5 to 80 MHz, passband insertion loss ≤ 1 dB, 30 dB stopband loss and return loss ≥ 15 dB at 50 ohms impedance. I felt that 30 dB stopband insertion loss above 88 MHz (the low end of the FM broadcast band) and below 1.705 MHz (high end of the AM broadcast band) would provide a reasonable compromise in the passband-to-stopband transition regions of the filter response.

Based on the above requirements, I selected the Mini-Circuits SXHP-5+ highpass, SXLP-90+ lowpass and BSF-C100+ bandstop filter modules. I chose the BSF-C100+ bandstop filter rather than the BSF-C88108+. The latter is designed specifically for the FM broadcast band and introduced too much loss in the desired passband. All three filter modules are catalog items, thus simplifying the project. The total material cost of the filter modules is about 67 USD. The composite filter is a *reflective* type in which incoming RF energy in the stopbands is reflected back and not absorbed.

Connecting individual filters in a cascade does not always yield expected good results. However, if the individual filters are well-designed and -built, success is more probable. As an initial step, I check the measured scattering parameters (S-parameters) for the individual filters, which may be downloaded from the manufacturer's website [{Mini-Circuits}](#). The S-parameter files may be combined in a circuit simulator to see how the individual filters interact with each other when in a cascade. This initial check can save considerable time and trouble. In the case of the filters used here, the circuit simulations showed good results and are discussed in section 4. A block diagram of the composite filter shows its simplicity while its functional schematic is only a little more complicated (figure 3).

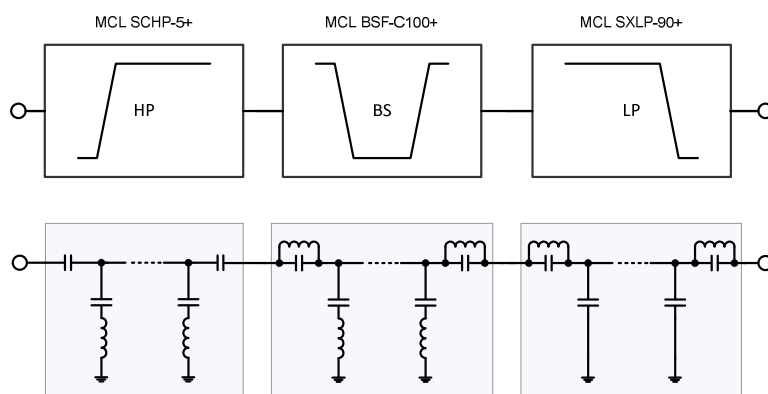


Figure 3 ~ Filter block diagram showing the individual filter modules immediately above their functional schematics. The component values are not published by the manufacturer. Image © 2020 W. Reeve

3. Printed Circuit Board

I designed the filter printed circuit board (PCB) in Target 3001 PCB design software from Germany and had the boards manufactured by JLCPCB in China (figure 4). The board unit cost is about 3 USD, and its dimensions and

shape are based on mounting in the milled aluminum enclosures that were on-hand. The three filter modules are hand-soldered to the PCB. Connections to the SMA-female RF connectors on the ends of the enclosure are through short (8 mm) tinned copper pigtailed soldered to turret terminals on the PCB (the enclosures do not allow direct mounting of the RF connectors on the PCB). The pigtailed introduce a small inductance at the filter input and output but do not seem to degrade overall performance. The finished filter is mechanically simple (figure 5).

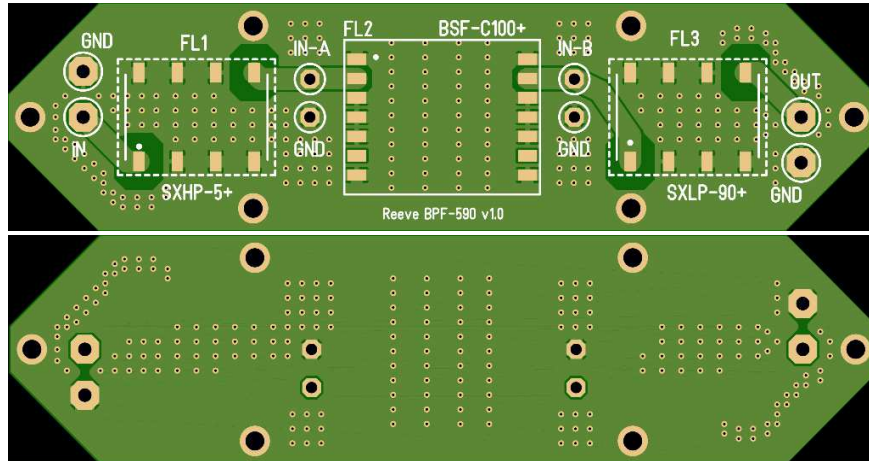


Figure 4 ~ Filter printed circuit board top and bottom images shown at 100% scale. The PCB has six mounting holes and the corners are trimmed to fit the milled aluminum enclosure. I included pads for plated metal turret terminals to be used for external connections and testing. These images are produced from the PCB Gerber (definition) files. Image source: JLCPCB

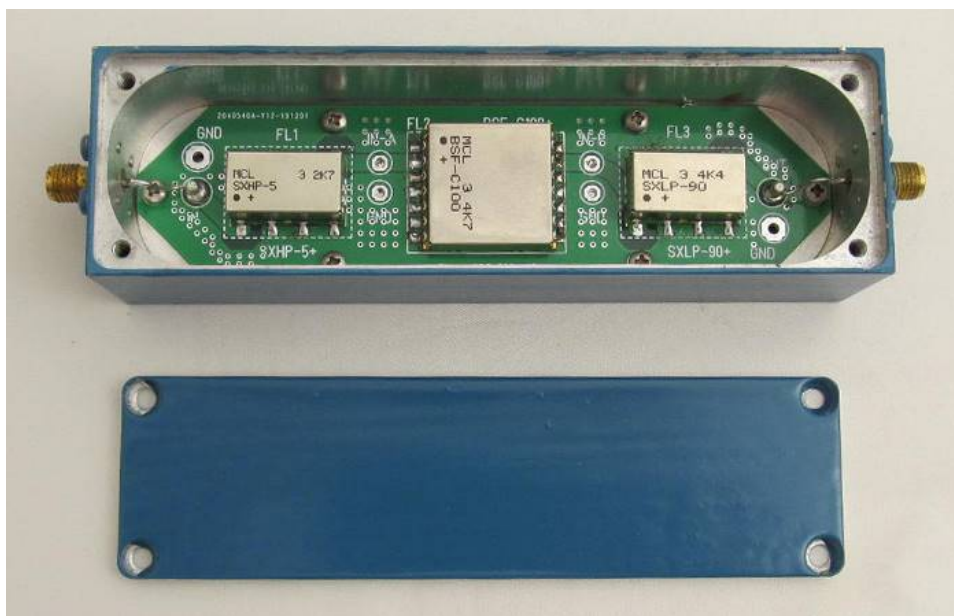


Figure 5 ~ Milled aluminum enclosure with the finished printed circuit board installed. The PCB is fastened with six 3-48 machine screws and lock washers, which bond the PCB ground reference plane to the enclosure. Image © 2020 W. Reeve

4. Filter Simulation and Measurements

The plots in this section were produced with {AppCAD}, a free circuit simulation software package by Avago Technologies. The software can cascade and display up to six 2-port S-parameter files, but it cannot display the calculated cascade along with a separate, singular composite file from measurements. It also cannot save a calculated cascade for later comparison to another file. Therefore, several plots are shown below of different combinations of S21 transmission coefficient and S11 reflection coefficient parameters that allow examination of the characteristics of the filter and the modules used in it. All plots are from 1 to 300 MHz:

- ⚙ Manufacturer’s S21 parameters for the individual filter modules (figure 6);

- ⚙ Calculated S21 parameters for the composite (cascaded) filter (figure 7);
- ⚙ Measured S21 parameters for the actual filter overlaid with individual module parameters from the manufacturer's files (figure 8);
- ⚙ Measured S21 parameters for the actual filter by itself (figure 9);
- ⚙ Manufacturer's S11 parameters for the individual filter modules as well as the measured S11 parameters for the actual composite filter (figure 10).

The completed filter was measured with a Keysight N9917A FieldFox Microwave Analyzer in Network Analyzer mode (some comparative measurements using another vector network analyzer are provided in section 5). Prior to the measurements, the network analyzer was calibrated with an Agilent 85033D 3.5 mm Calibration Kit and two 1 m long Bracke Manufacturing BM95003 precision cables. These cables have type N-male connectors on the test equipment end and type SMA-male connectors on the device under test (DUT) end, so no adapters were required. The calibration plane was established at the cable's SMA connectors, which were then installed on the filter for the measurements. The measurements were averaged and saved as a 2-port scattering parameter file (*.s2p). A tabulation compares the design goals and actual measured results (table 1).

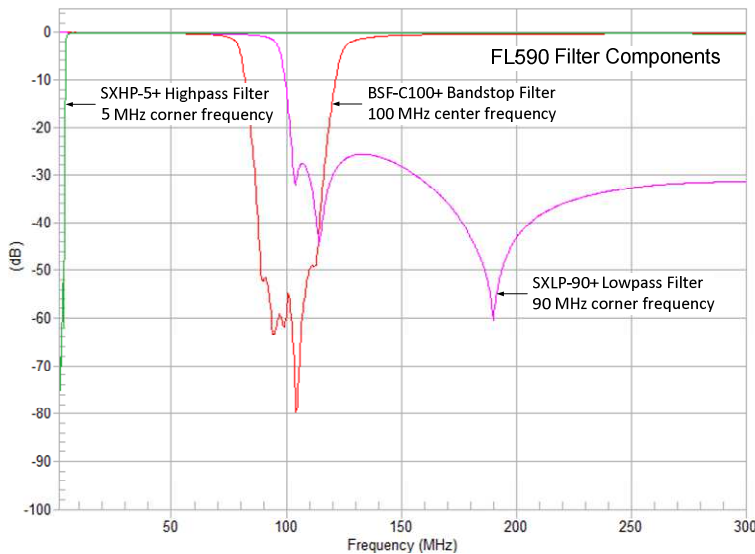


Figure 6 ~ Plots of the S21 scattering parameters for each individual filter module: Green trace: SXHP-5+ highpass filter, Red trace: BSF-C100+ bandstop filter, and Magenta trace: SXLP-90+ lowpass filter. The scattering parameters are provided by Mini-Circuits and most likely represent average values from measurements of numerous filters in a laboratory environment.

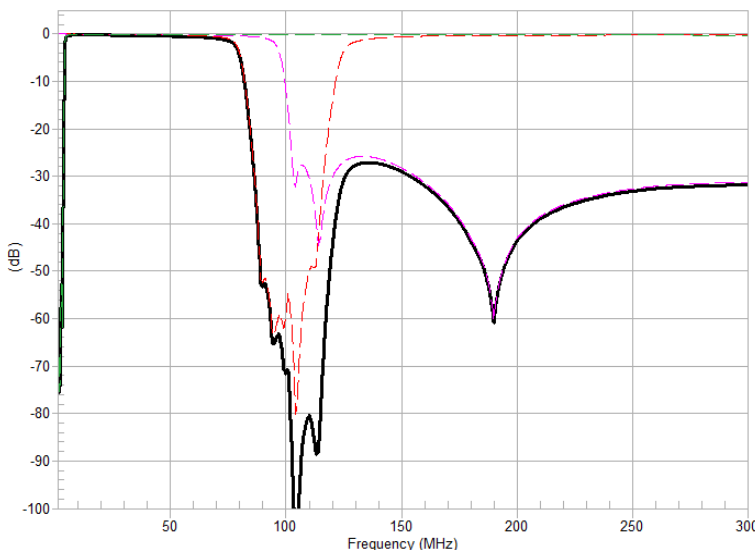


Figure 7 ~ Plots of the cascaded S21 scattering parameters (solid black trace) and for each individual filter module (dashed traces) as shown in the previous figure. All plots are based the filter manufacturer's data and not measurements. The plot of the cascaded S-parameters does not take into account implementation losses associated with installation of the modules on a PCB, mounting in an enclosure and connecting to external RF connectors. Compare the cascaded plot to the actual measurements of figure 7 or 8.

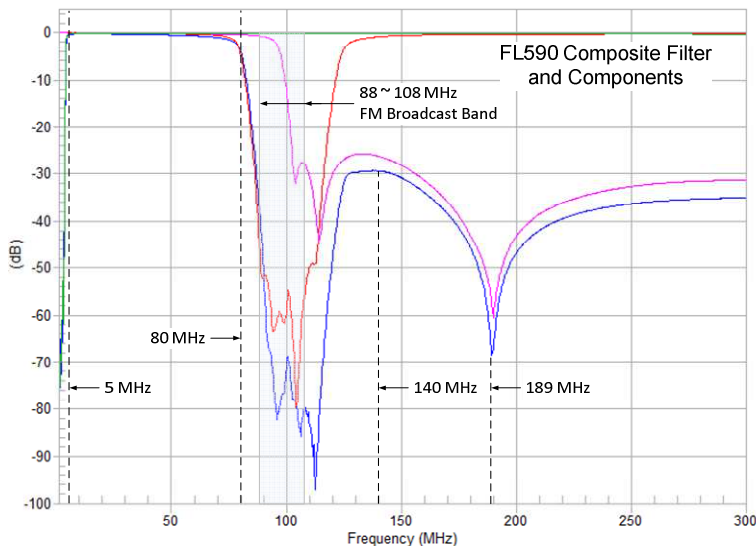


Figure 8 ~ Plots of the manufacturer's S21 transmission coefficient for each individual filter (green red and magenta traces) overlaid with the measured scattering parameters for the actual filter (blue trace). A few specific frequencies are indicated by callouts. The FM broadcast band is shown lightly shaded.

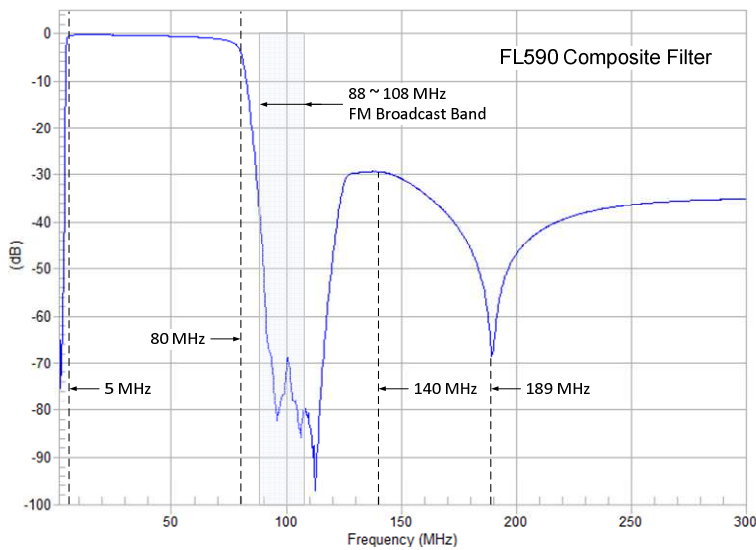


Figure 9 ~ Measured filter S21 transmission coefficient of the completed filter without the clutter of the individual parameters. The only obvious difference between this plot and figure 7 is in the stopband above about 90 MHz and these are insignificant. Some differences could be due to the frequency resolutions of the manufacturer's data compared to the measured data.

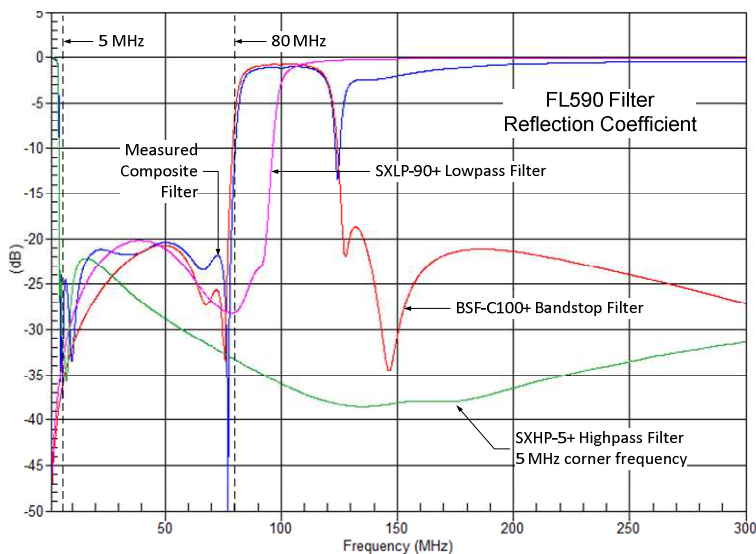


Figure 10 ~ Plots of the manufacturer's S11 reflection coefficient for each individual filter (green, red and magenta traces) overlaid with the measured S11 for the actual composite filter (blue trace). Of interest is the reflection coefficient for the composite filter passband from 5 to 80 MHz. The worst-case is -20.4 dB, which is equivalent to a return loss of $+20.4$ dB and a VSWR of 1.21: 1.

Table 1 ~ Comparison of FL590 design goals with measurements.
Individual values are based on marker measurements.

Parameter	Design	Measured
Insertion loss, 5 ... 80 MHz	≤ 1 dB	≤ 1 dB at 5 ... 72 MHz 3.2 dB at 80 MHz (worst-case)
Insertion loss, ≥ 88 MHz	≥ 30 dB	32.6 dB at 88 MHz 79 dB at 98 MHz 30.4 dB at 137 MHz (worst-case to 300 MHz)
Insertion loss, ≤ 1.7 MHz	≥ 30 dB	68.7 dB at 1705 kHz 59.9 dB at 900 kHz (worst case to 300 kHz) 62.1 dB at 535 kHz
Return loss, 5 ... 80 MHz	≥ 15 dB	≥ 20.4 dB (worst-case)

5. Comparative VNA Measurements

The measurements discussed in the previous section were made with an analyzer designed for professional field use. I thought it would be interesting to compare those to measurements with an instrument designed for amateur use, the DG8SAQ VNWA-3E. I previously wrote about this unit in [{ReeveFilt}](#).

Before using the VNWA-3E for measurements, I performed an SOLT (Short-Open-Load-Thru) calibration with the *Magi-Cal* automated electronic calibrator from [{SDR-Kits}](#). The calibration plane was established at the end of two 230 mm long RG-223 jumper cables supplied with the Magi-Cal. These cables have straight SMA-female connectors on one end and right-angle SMA-female connectors on the other. The calibrator and filter were connected to the end with the right-angle connectors. As with the N9917A, I averaged and saved the S-parameters produced by the VNWA-3E. I then imported both the N9917A and VNWA-3E files into the AppCAD application for viewing (figure 11 and 12). The differences are negligible.

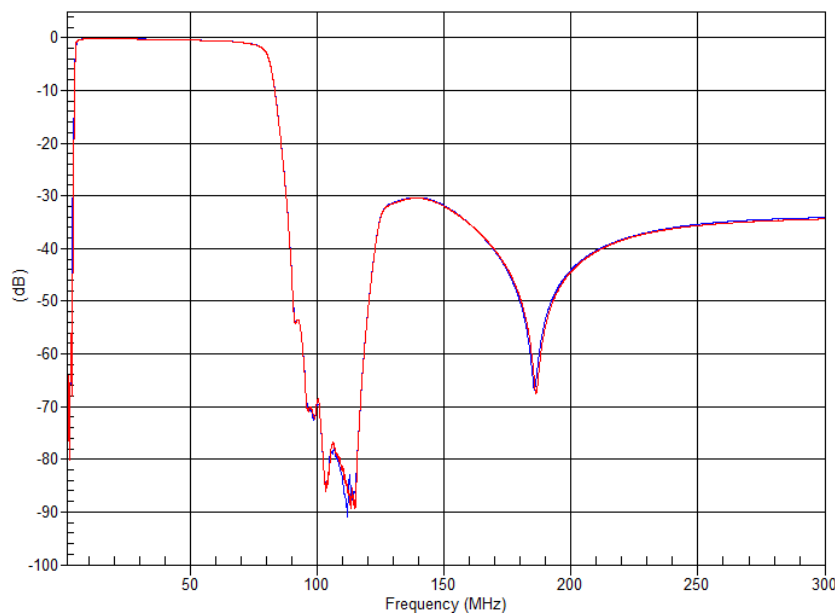


Figure 11 ~ Comparative S21 transmission coefficient measured by two network analyzers. Blue trace: N9917A; Red trace VNWA-3E. For practical purposes, the two traces are indistinguishable. The two plots were produced from measured data with the same frequency resolution.

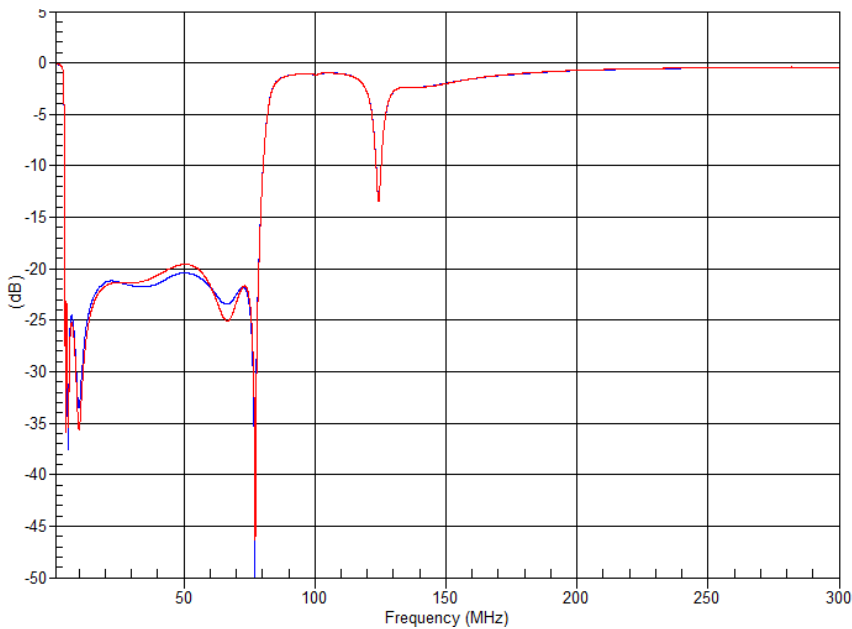


Figure 12 ~ Comparative S11 reflection coefficient measured by two network analyzers. Blue trace: N9917A; Red trace: VNWA-3E. The only discernible differences are in the passband and are less than 1 dB.

6. Performance

All filter measurements discussed above were made under laboratory conditions with 50 ohm terminations. Filters seldom are used under those conditions. At the beginning of [{ReeveBasFilt}](#) I provided three plots from an N9342C Handheld Spectrum Analyzer (HSA) that was connected to an outdoor VHF log periodic dipole array antenna pointed south. Three different bands were displayed – AM broadcast band, FM broadcast band and a 2 GHz band that was centered on 1.00025 GHz and encompassed the two broadcast bands as well as the television broadcast and cellular radio bands.

The measurements described in the previous paragraph were taken in late December 2017. At the time, I planned to compare the same conditions with various filter types connected between the antenna and spectrum analyzer. The first set of comparative measurements, which are discussed in this section, involves the FL590 (figure 13). It is interesting that the displayed integrated power levels without the filter are almost identical to the measurements in 2017.

The spectrum analyzer was setup exactly as before. For reference, a block diagram shows the measurement setup (figure 14). A set of new measurements were taken first without the filter and then with the filter in late February 2020, about 2 years after the previous measurements. The filter is reasonably well-matched to the antenna above 50 MHz (the measured antenna VSWR from 50 to 1000 MHz is $\leq 2:1$) but is very poorly matched below 50 MHz. Nevertheless, the filter appears to work well at the lower frequencies.

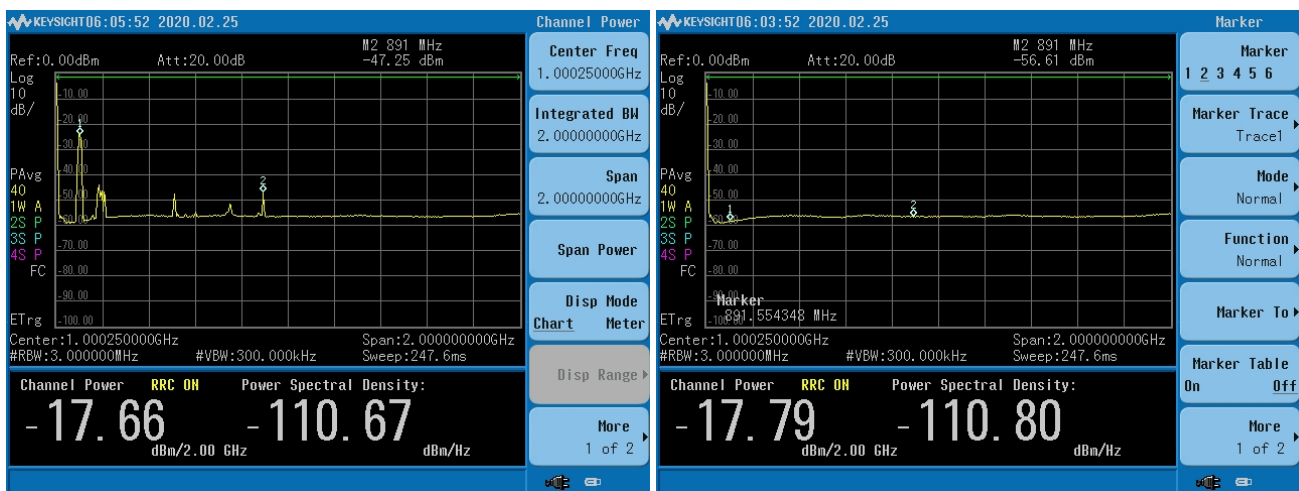
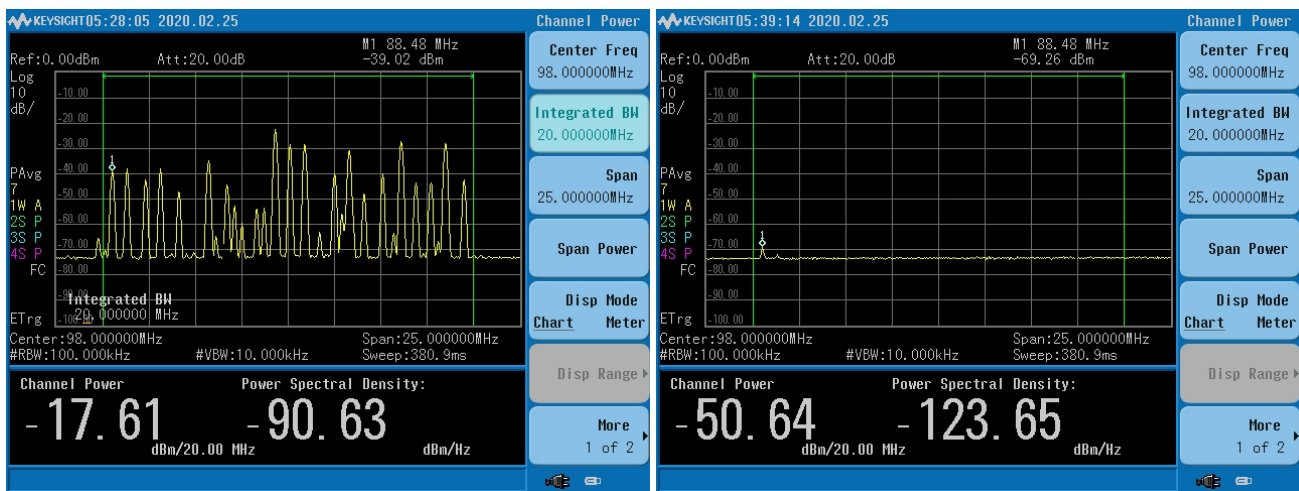
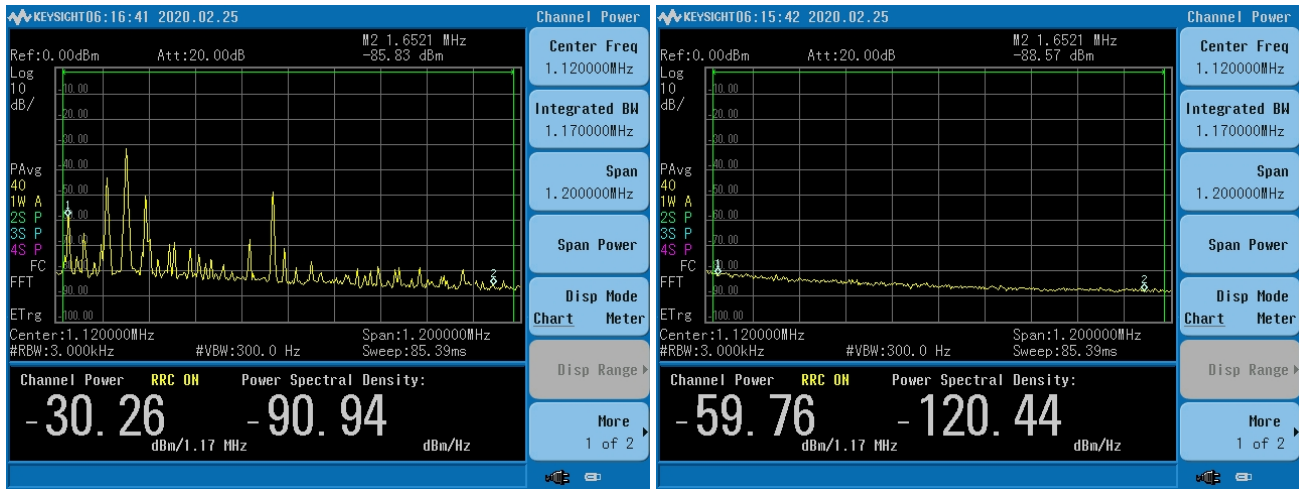


Figure 13 ~ Spectrum measurements without (left column) and with (right column) the FL590 filter for the AM broadcast band from 535 to 1705 MHz (top row), FM broadcast band from 88 to 108 MHz (middle row) and broadband from 250 kHz to 2 GHz (bottom row). The measurements without the filter show very closely the same integrated power levels as in [\[ReeveBasFilt\]](#), which were measured 2 years earlier. Except for one FM broadcast station at 88.5 MHz, all the stations have been completely eliminated by the filter to at least the displayed noise floor. The one remaining station is KAKL with 11 kW effective radiated power about 9 km south and well within of the receive antenna pattern. Note that, in the spectra for the AM and FM broadcast bands, the signals dominate the integrated power levels in the bandwidths selected and the filter

reduces the measured power levels. However, in the 2 GHz wideband spectra, the spectrum analyzer noise dominates and the filter introduces negligible reduction in the measured integrated power level but it does reduce the individual signals.

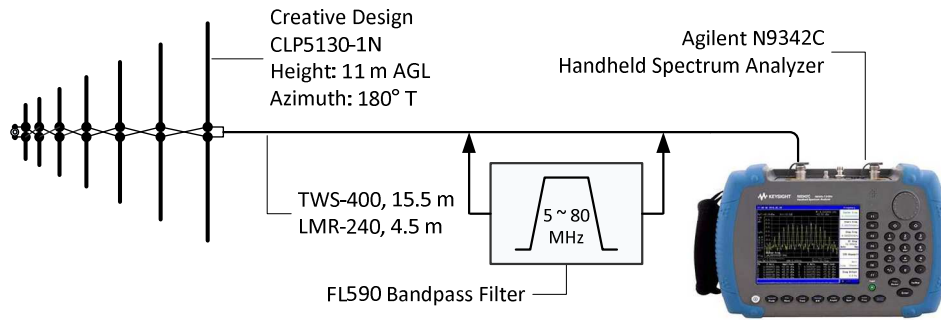


Figure 14 ~ Block diagram for the measurements. The antenna is a 21-element LPDA with frequency range 50 to 1300 MHz. After baseline measurements, the FL590 filter was inserted inline with the antenna feedline to the spectrum analyzer. Image © 2020 W. Reeve

The noise floor seen in the above spectrum images is determined mostly by the resolution bandwidth (RBW) setting, which must be fairly wide for the integrated power measurements. To give a better idea of the filter’s performance, I increased the spectrum analyzer sensitivity by reducing the RBW to 100 Hz for the 25 MHz frequency span around the FM broadcast band (100 kHz RBW was previously used in this band). I also turned on the Preamplifier, which substantially improves the analyzer noise figure, and changed the reference level from 0 dBm to -40 dBm. I then made additional measurements at these settings without and with the FL590 filter (figure 15).

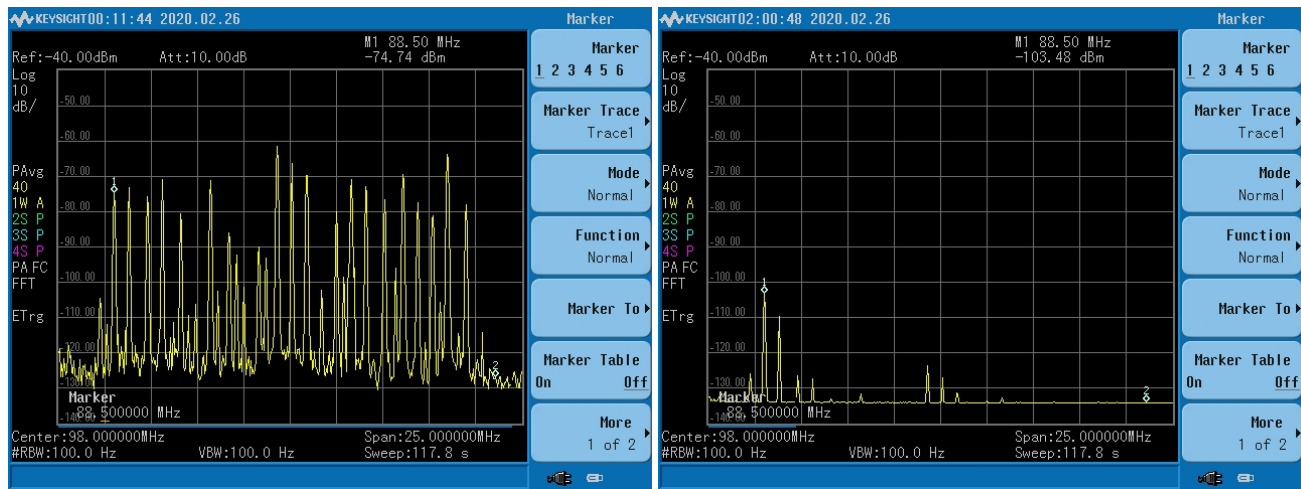


Figure 15 ~ High sensitivity spectrum measurements of the FM broadcast band without (left) and with (right) the FL590 filter. The RBW was set to 100 Hz, which yielded a -133 dBm displayed noise floor. Note that the station at 88.5 MHz is the strongest after filtering (see text), and its level has been reduced 28.8 dB from -74.7 dBm to -103.5 dBm.

Unlike the integrated power measurements, with their relatively high noise floor, the measurements at the higher sensitivity indicate the filter does not completely eliminate interfering signals in the FM broadcast band, especially stations within view of the antenna main lobe at the lower end of the band. Based on the measurements in sections 4, this is expected because stations at the low end of the band experience less filter loss than the middle and high ends of the band.

7. Applications

One of the main applications for the FL590 filter is in the front-end of an up-converter for the LWA antenna when used with the Callisto solar radio spectrometer. The Callisto instrument's native frequency range is 45 to 870 MHz, which straddles only about one-half of the LWA frequency range. When the Sun is active, many solar radio bursts extend down to frequencies in the HF band and lower VHF band, below the Callisto's native frequency range.

Earth's ionosphere often blocks celestial emissions below about 15 MHz, but there are times when emissions as low as 5 MHz can be received. Thus, an up-converter with the FL590 filter allows the Callisto to observe the lower frequencies while reducing the effects of terrestrial radio interference from outside the observation frequency band. A dual converter and Callisto installation are needed to take advantage of the LWA antenna's two polarizations.

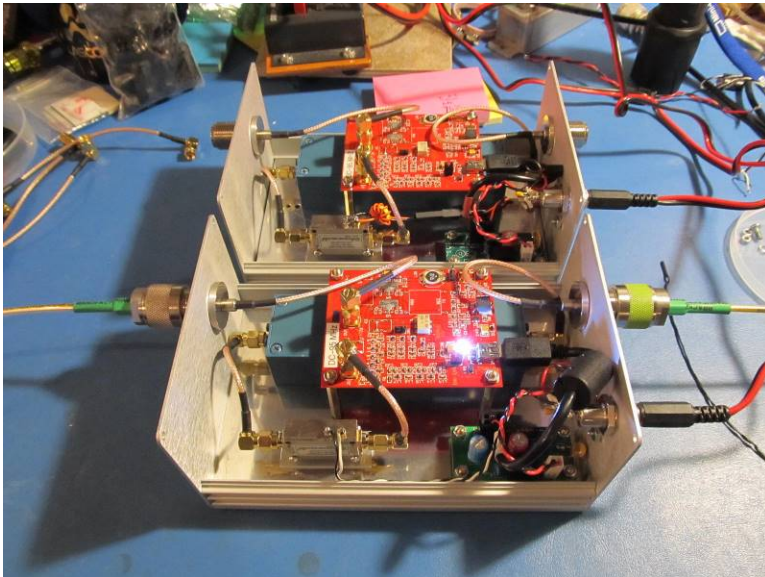


Figure 16.a ~ Two identical experimental up-converters shown without covers while under test. The filter is visible underneath the red mixer/local oscillator mezzanine PCB. The mixer/oscillator PCB includes lumped element filters for the oscillator output and IF output but has no shielding. Included on the chassis are a small power supply PCB (lower-right in the enclosure) with 5 and 12 Vdc outputs, and a Wenteq low noise amplifier (lower-left in the enclosure). Two up-converters are needed with the LWA antenna because of its dual polarization. Image © 2020 W. Reeve

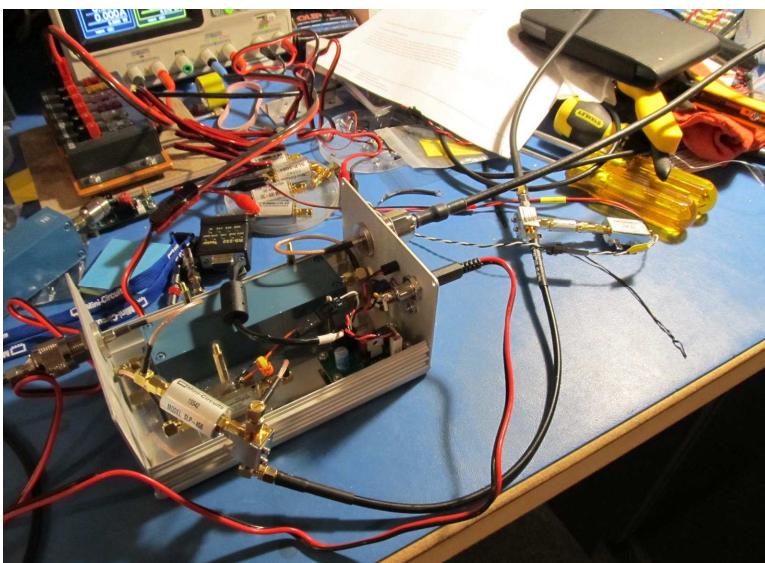


Figure 16.b ~ Another experimental up-converter prototype in a rat's nest configuration with one FL590 filter mounted on the enclosure base chassis and connected to the RF input of a shielded double-balanced mixer module. The version shown here uses a single fixed-tuned VCO for the local oscillator (middle-right of image outside of the enclosure near the two screwdrivers) connected to a 2-way splitter. One leg of the splitter goes to the LO input of the mixer (lower-left hanging off the edge of the enclosure) and the other leg goes to a frequency counter (not visible). The concept proved workable so a final prototype was built with all components in a single enclosure (next figure). Image © 2020 W. Reeve



Figure 16.c ~ Final prototype of the experimental up-converter built with two aluminum chassis layers. The enclosure is the same as used with the Callisto instrument. The bottom chassis (not visible) holds two FL590 filters and has space for two input amplifiers (not installed here because amplifiers are not needed with the LWA antenna). The upper chassis holds two shielded mixers, an oscillator, splitter and three filters for the oscillator and IF outputs. Two identical converters are built in one enclosure and share the oscillator. This proved to be a good design and will be manufactured after selecting the LO frequency (see text). Image © 2020 W. Reeve

The FL590 filter has been installed in several experimental up-converter designs. One has a 200 MHz local oscillator, which provides an intermediate frequency (IF) output range from 205 to 280 MHz (figure 16.a). Another experimental model is based on completely shielded mixers and a shared local oscillator (figure 16.b). A final prototype has all components packed together (figure 16.c). For this converter, the LO will be selected to operate at a fixed frequency somewhere between 230 and 320 MHz. For a 230 MHz LO, the IF output range would be 235 to 310 MHz, and for a 320 MHz LO, the IF output would be 325 to 400 MHz. This frequency plan avoids the television broadcast band where radio frequency interference is possible from strong broadcast transmitters and places it in the military aviation band. The actual oscillator frequency will be determined during testing and chosen based on spurious signal performance.

8. Conclusions

A passband filter has been designed for the LWA antenna with a frequency range of 5 to 80 MHz. The filter is based on surface mounted highpass, lowpass and bandstop filter modules produced by Mini-Circuits and will be used in up-converters for the Callisto spectrometer. The filter modules are installed on an in-house-designed printed circuit board, which is mounted in a repurposed machined aluminum enclosure. Measurements show that the filter meets the overall electrical design performance requirements.

9. Weblinks and References

- {AppCAD} <http://www.hp.woodshot.com/>
- {Mini-Circuits} <https://www.minicircuits.com/>
- {ReeveBasFilt} http://www.reeve.com/Documents/Articles%20Papers/Reeve_BasicFilters.pdf
- {ReeveFilt} http://www.reeve.com/Documents/Articles%20Papers/Reeve_FilterMeasVNA.pdf
- {ReeveLWA} http://www.reeve.com/RadioScience/Antennas/ActiveCrossed-Dipole/LWA_Antenna.htm
- {SDR-Kits} https://www.sdr-kits.net/Magi-Cal-Automated_SMA_Calibrator_for_VNWA



Author: Whitham Reeve is a contributing editor for the SARA journal, Radio Astronomy. He obtained B.S. and M.S. degrees in Electrical Engineering at University of Alaska Fairbanks, USA. He worked as a professional engineer and engineering firm owner/operator in the airline and telecommunications industries for more than 40 years and now manufactures electronic equipment used in radio astronomy. He has lived in Anchorage, Alaska his entire life. Email contact: whitreeve@gmail.com

Document information

Author: Whitham D. Reeve

Copyright: © 2020 W. Reeve

Revision: 0.0 (Original draft started, added S21 plots, 30 Jan 2020)
0.1 (Added S11 plot, 31 Jan 2020)
0.1 (Added filter and PCB images, 11 Feb 2020)
0.2 (Added comparative measurements, 12 Feb 2020)
0.3 (Added Applications section, 13 Feb 2020)
0.4 (Replaced comparative plots, 14 Feb 2020)
0.5 (Added Performance section, 24 Feb 2020)
0.6 (Completed 1st draft, 25 Feb 2020)
0.7 (Added conclusions, 22 Mar 2020)
0.8 (Completed 2nd draft, 02 Apr 2020)

Word count: 3549

File size: 2846208